Effective temperatures and surface gravities of OB-stars derived from synthetic photometry

Simon Grosse-Holz

Supervisor: Dr. Andreas Irrgang, Prof. Dr. Ulrich Heber

Abstract

In this work, we developed an algorithm for estimation of effective temperature T_{eff} and surface gravity $\log g$ of OB-type stars from observations in different photometric systems. The algorithm was implemented and tested using synthetic spectra whose creation parameters could be reproduced accurately.

November 24, 2014

Contents

1 Introduction

Photometry is one of the easiest ways to quantitatively analyse the light of stars. On doing so several band-pass filters are used, "cutting" some (filter specific) color out of the spectrum of the starlight. The brightness of this color (in the following called "magnitude") is then measured. Practically this can be done very easily and with high temporal resolution (compared to recording and analysing the whole spectrum). Thus this method is widely used to obtain information about astronomical objects. Plotting the magnitude over time, one can determine the period of a binary star or search for exoplanets for example. For single stars the magnitudes are not time dependent and can provide the observer with information about the type of star via the Hertzsprung-Russell diagram.
Nowadays often also synthetic photometry is used to determine the stellar parameters more precisely. Synthetic photometry means modelling the physical processes which determine the starlight's evolution until the observation and then adjusting the models until the predicted magnitudes coincide with the observations. This yields results for the parameters included in the model, which are for example effective temperature T_{eff} and surface gravity g.
A program for these computations was written before by Napiwotzki et al. [1993] for the commonly used Strömgren $uvby\beta$-system of filters. Here we aimed at including more (arbitrary) filter systems, e.g. Johnson UBV-system, or the $ugrzi$-system used by the Sloan Digital Sky Survey. Furthermore the advantages of self-written code are modifiability and adaptability to existing code, so this project (hopefully) provides my supervisor Dr. Andreas Irrgang with a useful tool for his further work.

2 Terminologies

2.1 General astronomical terminologies

The *effective temperature* T_{eff} of a star is defined as the temperature of a black body emitting the same total amount of radiation. This is the commonly used notion of temperature for stars, thus it is also often just called temperature of the star.
The *surface gravity* g of a star is measured in cgs-units (which is here $\frac{\text{cm}}{\text{s}^2}$) and used logarithmically, abbreviated commonly with $\log g$, meaning $\log(g \cdot \frac{\text{s}^2}{\text{cm}})$. For comparison one may think of the earth's surface gravity $g = 9.81\,\frac{\text{m}}{\text{s}^2}$ giving $\log g \approx 3$.
In general, in astronomy the symbol log is meant to be the logarithm to base 10 (instead of e as common elsewhere).

2.2 Spectroscopical terminologies

In spectroscopy, the *spectrum* of a star (precisely: the spectrum of the star's light) is recorded and analysed. In this spectrum, one plots the electromagnetic *flux* f over the wavelength λ. Physically correct the so called flux is the flux density over the wavelength, but in spectroscopy this is normally just called flux. It is defined as radiative power per unit area and wavelength.
The *intensity* I is defined as radiative power per unit area. Comparison with the flux gives

$$\int f \,\mathrm{d}\lambda = \frac{\mathrm{d}P}{\mathrm{d}A} =: I \,. \tag{1}$$

The intensity is the quantity that is measured when recording photometric magnitudes (see below).
Due to the distance of the star being observed, we have to do a *flux correction*. Let F (as for example given by the computed synthetic spectra, see below) denote the flux emanating from the star's surface $4\pi R^2$ where R is the radius of the star. Then using (1) we get the radiative power P_{rad} of the star by

$$P_{\mathrm{rad}} = \iint F \,\mathrm{d}\lambda \,\mathrm{d}A = \int I_{\mathrm{rad}} \,\mathrm{d}A = 4\pi R^2 I_{\mathrm{rad}} \,, \tag{2}$$

where a homogeneous intensity distribution over the star's surface was assumed in the last step.
As the light moves in any direction with the same speed and energy is conserved, in a distance d from the star the energy radiated from the star's surface in one unit time interval (the power) is now distributed to a sphere with radius d and thus surface area $4\pi d^2$, leading to a reduced intensity I_{d}. The same consideration as in (2) yields $P_{\mathrm{rad}} = 4\pi d^2 I_{\mathrm{d}}$. Equating this with (2) one obtains

$$4\pi R^2 I_{\mathrm{rad}} = P_{\mathrm{rad}} = 4\pi d^2 I_{\mathrm{d}} \;\Leftrightarrow\; I_{\mathrm{d}} = \frac{R^2}{d^2} I_{\mathrm{rad}} = (\tfrac{1}{2}\theta)^2 I_{\mathrm{rad}} \,, \tag{3}$$

where $\theta = \frac{2R}{d}$ is the angular diameter of the star (assuming $R \ll d$).
Assuming that the spectral distribution does not change, we can derive the flux f at the distance d as

$$f = (\tfrac{1}{2}\theta)^2 F \,. \tag{4}$$

2.3 Photometrical terminologies

As already mentioned, photometry is about measuring the intensities of starlight shining through different *filters*. These filters are normally grouped to *filter systems* containing several filters transparent for different parts of the electromagnetic spectrum. What part of the spectrum the filter is transparent for is specified by the *filter function*.
This function also includes the response of the detection device and therefore differs in definition whether an energy integrating (e.g. a photomultiplier) or a photon counting (e.g. a CCD) device is used. As the published filter functions

assume photon counting devices, we did so too. This results in the filter function being defined at some wavelength λ as the output signal of the instrument per incoming photons with wavelength λ. (Usually the filter functions are normalized to meet some requirement, for example that the integral over λ equals 1 or that the peak value is 1). This sort of filter function is also called *photonic passband*.
The assumption of photonic passbands has to be regarded when computing intensities (e.g. in (7)). According to (1) the intensity can be written as

$$I = \int f(\lambda) S'(\lambda)\,\mathrm{d}\lambda =: \langle f \rangle \tag{5}$$

where $S'(\lambda)$ gives the percentage of **energy** coming through the filter. But as defined above, the function $S(\lambda)$ gives the output signal of our instrument per incoming **photons**. But the spectroscopic flux f again is in units of energy. Obviously using the Planck-Einstein-relation $E_\mathrm{p} = \frac{hc}{\lambda}$ we can convert f to the photon flux n_p via $n_\mathrm{p}(\lambda) = \frac{f(\lambda)}{E_\mathrm{p}(\lambda)} \propto f(\lambda)\lambda$. Now we get the mean photon flux $\langle n_\mathrm{p} \rangle$ by $\langle n_\mathrm{p} \rangle = \int n_\mathrm{p}(\lambda) S(\lambda)\,\mathrm{d}\lambda$ and according to Bessell and Murphy [2012] (equation A13), this is proportional to the mean energy flux $\langle f \rangle$, giving

$$I \overset{(5)}{=} \langle f \rangle \propto \langle n_\mathrm{p} \rangle \propto \int f(\lambda) S(\lambda) \lambda\,\mathrm{d}\lambda\,. \tag{6}$$

As we normally (see (7)) just look at quotients of intensities, we do not have to worry about the proportionality constants here.
Unfortunately this paragraph had to be a little technical in order to simplify the next one.
The measured quantities in photometry are *magnitudes* and *colors*, named like the corresponding filter (e.g. "the Johnson V magnitude" means the intensity measured with the V filter of the Johnson system).
A magnitude m is the intensity of starlight (eventually filtered by some filter), measured logarithmically in comparison with some *reference star* (usually Vega):

$$m := -2.5 \log\left(\frac{I}{I_\mathrm{ref}}\right) + m_\mathrm{ref} \overset{(6)}{=} -2.5 \log\left(\frac{\int f(\lambda) S(\lambda) \lambda\,\mathrm{d}\lambda}{\int f_\mathrm{ref}(\lambda) S(\lambda) \lambda\,\mathrm{d}\lambda}\right) + m_\mathrm{ref} \tag{7}$$

$$= -2.5 \log \int f(\lambda) S(\lambda) \lambda\,\mathrm{d}\lambda \underbrace{-2.5 \log \int f_\mathrm{ref}(\lambda) S(\lambda) \lambda\,\mathrm{d}\lambda + m_\mathrm{ref}}_{=: m_\mathrm{ZP}} \tag{8}$$

where $f(\lambda)$ is the incoming flux, $S(\lambda)$ is the filter function, $f_\mathrm{ref}(\lambda)$ is the flux of the reference object and m_ref is the corresponding magnitude of the reference object. m_ref is actually just definition (i.e. the Johnson V magnitude of Vega for example is defined to be 0.027). Sometimes the reference flux and magnitude are combined (as in (8)) to give the *zero point magnitude* m_ZP. The factor of -2.5 and the reference magnitudes are historically induced; notice the minus sign, which results in smaller magnitudes representing higher intensities and vice versa.

Here we want to distinguish between the notion of a *magnitude*, which is explained above, and a *color*. A color is a difference of two magnitudes, the Johnson $U - B$ color is a common example. Using these colors, one can obtain information about the distribution of the flux in one part of the spectrum relative to another part (remember that the magnitude scale is logarithmic: a difference in magnitudes corresponds to a quotient in intensities). Sometimes also further constructions like differences of colors are used, which for simplicity we will also call colors (or indices). One example is the c_1 index of the Strömgren $uvby\beta$-system being computed as $c_1 = (u - v) - (v - b)$.
One application of colors is *interstellar reddening*. The light emitted from a star has to travel through space to reach the earth. On its way, it meets interstellar dust and similar matter, modifying the spectral distribution: When the light hits dust particles, some energy-rich blue photons are scattered at the particles and therefore losing energy, which increases the wavelength. Thus some of the flux from the blue part of the spectrum is shifted redwards. This process is called interstellar reddening and its effect obviously is the larger, the more matter the light meets on its way. As measure for interstellar reddening we used the color excess $E(B - V)$ of the Johnson $B - V$ color. This color excess is defined as the difference of the "intrinsic" (the emitted) $B - V$ color and the observed (thus "reddened") color. As interstellar reddening shifts flux from the blue part (represented by the B filter) to the red part (represented by the V filter), $B - V$ should grow with increasing reddening (remember the minus sign in the definition of a magnitude). Thus it suits as a measure for reddening. To achieve comparability amongst different stars which might have different $B - V$ intrinsically, this intrinsic value is subtracted, giving the definition above.

3 Synthetic photometry

As mentioned in section 1, synthetic photometry is about modifying model parameters such that the predicted magnitudes match the observed ones. Here I will give a short explanation of the used models, which aim at simulating the light's evolution from creation in the star until the observation.
We begin with a model atmosphere for the observed star. This model contains the parameters effective temperature T_{eff} of the star, its surface gravity $\log g$, abundances of several elements and things like turbulences in the atmosphere. From this model, the spectrum of the star can be computed. Such a computed spectrum is called a *synthetic spectrum*. This spectrum resembles the one emitted by the star, if the chosen model parameters resemble the ones really occurring in the observed star (assuming sufficient correctness of the model).
The next step is the light travelling through space to earth. As explained in section 2.3 this leads to interstellar reddening, measured by the color excess $E(B - V)$.
As the starlight reaches the earth it has to pass the earth's atmosphere, which obviously also has a big impact on the spectral distribution. This impact strongly depends on time and location of the observation and therefore is sup-

posed to be corrected for already in the observational data. Thus we do not have to consider this here.
By now, the model computation provides us with the spectrum of the star as it is supposed to reach the telescope. As mentioned above, photometry is about filtering the starlight. As the filter functions for the commonly used filter systems are published, the filtering step can easily be done numerically using (7). In this way one obtains the synthetic magnitudes for a fixed set of model parameters. These parameters are:

- Effective temperature T_{eff} and surface gravity $\log g$
- Chemical elemental abundances in the star‘s atmosphere
- Motion of the star and turbulences in its atmosphere
- The interstellar reddening, described as color excess $E(B-V)$
- The flux correction (see sect. 2.2) parametrized by the star‘s angular diameter θ

The elemental abundances in the star‘s atmosphere mainly give absorption lines in the spectrum, which are few to fractions of Ångströms in width. These are negligible compared to filters with around 100-1000 Å in width and therefore do not have a significant impact on photometric magnitudes. Neither do the star‘s motion nor the turbulences, so in this work we set all those parameters to standard values and did not change them. This leaves T_{eff}, $\log g$, $E(B-V)$ and θ as variables. Now we wrote a program that searches the best match of these parameters with the observational data and thus gives values for these variables, providing information about the star under consideration.

4 Implementation

4.1 Terminologies

The conclusion of section 3 was that we are left with the *parameters* T_{eff}, $\log g$, $E(B-V)$ and θ and now from these have to compute the synthetic magnitudes to compare them with the observations. The main part of this computation is the *fit function*, which takes said parameters and computes the synthetic magnitudes. By evaluating the fit function for several different sets of parameters, a standard *fit algorithm* can determine the set of parameters, that best matches the observations. This is the *optimal fit*.

4.2 Development of the algorithm

As we modified our algorithm several times, using different approaches on the modelling, I will shortly outline these different approaches here.

4.2.1 Straightforward modelling

The first approach was to model the processes straightforward as explained in section 3. This means writing the fit function as follows: first compute the synthetic spectrum from the input parameters, then do the flux calibration and interstellar reddening and last but not least compute the synthetic magnitudes using equation (7). The implementation for computing the synthetic spectra was previous to my project done by my supervisor Dr. Irrgang and thus not part of this work. For the interstellar reddening we used the so called *reddening curve* of Fitzpatrick [1999] giving a reddening correction r in units of magnitudes per color excess $E(B-V)$ as function of wavelength, ending up with the reddening-corrected flux f_{red} dependent on the incident flux f given as

$$f_{\mathrm{red}}(\lambda) = f(\lambda) \cdot 10^{-0.4 r(\lambda) E(B-V)} \,. \tag{9}$$

The term $10^{-0.4\,\cdots}$ corrects for the mentioned fact that the reddening is given in magnitudes, which (looking at (7)) includes some $-2.5 \log \ldots$.
This approach is very nice, because it directly resembles the physical processes and thus is easy to adopt to changing conditions. For example one could easily include also the elemental abundances as parameters, as these would then just have to be passed additionally to the function computing the synthetic spectrum. On the other hand, the computation of the synthetic spectra is also the biggest problem in this method, because it is very CPU-intensive. As the fit function is called many times by the fit algorithm, this leads to large computation times.

4.2.2 Using a grid

Because one possible application of this program is the fast estimation of T_{eff} and $\log g$ for many stars, we wanted to keep the computational cost for one run as low as possible. Thus our second approach was to compute a grid for fixed ranges of our parameters, where we listed the different magnitudes in dependence of the model parameters. For arbitrary parameter values the fit function then just has to interpolate between the grid points to obtain the corresponding synthetic magnitudes. This approach has the advantage of much less computational cost, as the expensive computation of the synthetic spectra is replaced by a cubic spline interpolation between the grid points.
The disadvantage is the fixed range of the parameters and the fixed values for all parameters that are not included in the grid. These are for example the elemental abundances, which have no big effect on the synthetic magnitudes, but are needed to compute the spectrum. Also the number of parameters to be included in the grid should be kept as low as possible, as each parameter increases the dimension of the grid by 1. So in principle, by having the four parameters T_{eff}, $\log g$, $E(B-V)$ and θ, we had to compute a four-dimensional grid. But looking at (4), (8), one sees that for the flux corrected magnitude m_{fc}

(as the factor $(\frac{1}{2}\theta)^2$ is constant over λ) we obtain

$$\begin{aligned} m_{\mathrm{fc}} &= -2.5 \log \int (\tfrac{1}{2}\theta)^2 f(\lambda) S(\lambda) \lambda \, \mathrm{d}\lambda + m_{\mathrm{ZP}} \\ &= -2.5 \log \int f(\lambda) S(\lambda) \lambda \, \mathrm{d}\lambda - 5 \log \tfrac{1}{2}\theta + m_{\mathrm{ZP}} \\ &= m - 5 \log \tfrac{1}{2}\theta \end{aligned} \tag{10}$$

where m is the magnitude without flux correction. Thus the computation of the magnitudes and the flux correction can be separated, which gives us the advantage of just having to compute a 3-dimensional grid and having θ as continuous parameter.

4.2.3 Further reduction of dimensionality

Our last approach modified the mechanism of reddening. Reading Fitzpatrick [1999] we realised that the derived reddening curve was based upon the reddening corrections for single magnitudes. As we actually wanted to use it not to compute reddened spectra, but reddened magnitudes, it seemed to us a little bit like running in a circle to use reddened magnitudes to compute a reddening curve to redden a spectrum from which then again the reddened magnitudes are computed. This is obviously not the direct approach that one would want to use and thus probably generating unnecessary errors. Also, if it was possible to redden the computed magnitudes instead of the whole spectrum, like for θ in the flux correction we could leave $E(B-V)$ as continuous parameter and reduce the dimension of the grid to 2.
Because we wanted to keep our approach general and not restrict ourselves to the Johnson and Strömgren systems used for the data of Fitzpatrick, we did not want to directly use the values given there. So we computed the values from our grid from the second approach, where we reddened the spectra using the complete reddening curve. Obviously, if m and m_{red} denote the unreddened and the reddened magnitudes respectively, the correction is $m_{\mathrm{red}} - m$. To obtain the values given by Fitzpatrick, we divided this by the corresponding value of $E(B-V)$, giving the general correction term. Now the reddening correction for a specified $E(B-V)$ can be obtained by multiplying the general correction term with $E(B-V)$. Thus we have eliminated the need to redden the spectrum and in this way can leave $E(B-V)$ as continuous parameter in the fit function.

5 Tests of the algorithms with synthetic spectra

In this section I want to show some computations done with my program and in this way confirm that it works like it is supposed to. The different algorithms explained in section 4.2 were tested with the following procedure:

1. Compute a synthetic spectrum with random initial parameters
2. Use the synthetic spectrum to compute synthetic magnitudes

3. Set the computed magnitudes as input values to the algorithm and see how good the initial parameters are reproduced

In the second step I also tested the two different approaches for the reddening correction: redden the spectrum prior to computing the magnitudes from it (in the following "spectrum reddening") vs. directly redden the magnitudes (in the following "magnitude reddening").
Here the three algorithms available (see section 4.2) will be referenced as follows: the first one (sec. 4.2.1) where no grid was used at all by "no grid", the second one (explained in sec. 4.2.2) by "3D grid" and the last one (sec. 4.2.3) by "2D grid".
This gives a total of six different ways to compute comparable results. For each of these ways a random sample of 500 "stars" (sets of random values for the four parameters T_{eff}, $\log g$, $E(B-V)$ and θ) was tested. Figure 1 gives a first glance at the results, table 1 gives the legend for the upcoming figures.

Table 1: The colors used in the following figures to label the different combinations of reddening the input magnitudes and computing the output parameter values.

	no grid	3D grid	2D grid
spectrum reddening	black	green	cyan
magnitude reddening	red	blue	magenta

5.1 Effective Temperature T_{eff}

As shown in figure 2, spectrum reddening in the fit function indeed gives a systematic error in temperature estimation. Also the effects of grid interpolation can be seen nicely.

Figure 3 shows that the deviation of the fitted temperature does not significantly depend on the initial $\log g$ value. Obviously there is also no "sinusoidal" systematic error due to the grid interpolation like for the dependence on the initial T_{eff}.

5.2 Surface gravity $\log g$

In fig. 4 the deviation of the fitted $\log g$ to the initial value is plotted against said initial value (same plot as fig. 2, just for $\log g$). Again one clearly sees the effect of using different reddening mechanisms. Also the grid interpolation apparently affects $\log g$ not as much as T_{eff}.

Fig. 5 we mainly see the interpretation of fig. 4 strengthened. Unfortuately here we also see an error for which there is no obvious explanation.

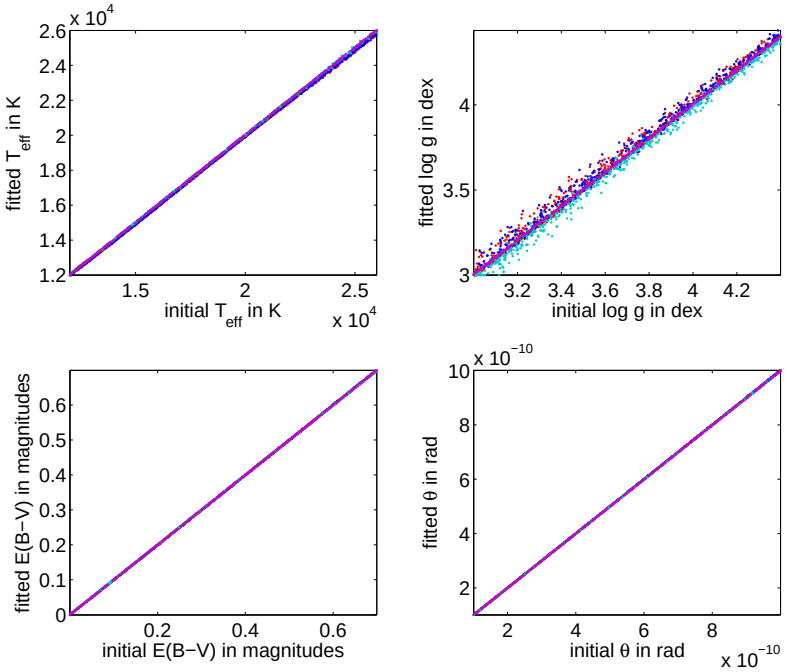

Figure 1: Fit results for the four input parameters. The different colors code for the different combinations of algorithms (see table 1 for explanation). Obviously all the parameters could be reproduced nicely. For further details see below.

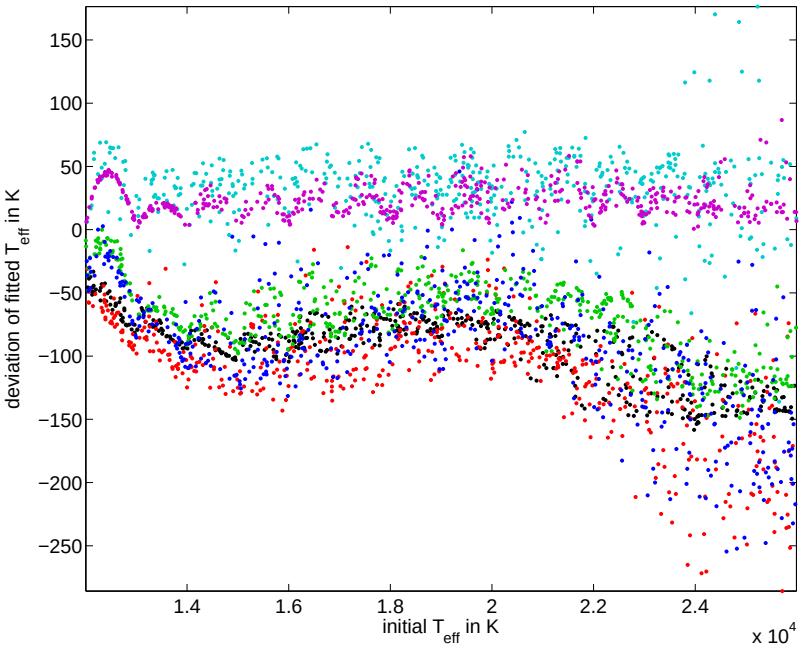

Figure 2: Deviation of the fitted T_{eff} depending on the initial temperature. In fact this is just a close up look of the plot in fig. 1 where the "ideal line" $T_{\text{eff,fit}} = T_{\text{eff,in}}$ was subtracted. See table 1 for color explanation.
Obviously there are two different trends: firstly (black, red, green, blue) the data from all the pairings of algorithms including spectrum reddening in the fit function (as do the "no grid" and the "3D grid" functions). These four curves mainly all show the same systematic error which therefore can be assumed to be due to the use of spectrum reddening in the fit function. Secondly the two curves for the "2D grid" fit function which uses magnitude reddening show a much better match with the initial parameters. But here one can also observe a systematic error, as especially the magenta curve (where magnitude reddening was used for generation of the input synthetic magnitudes) shows some strange "sinusoidal" behavior. Regarding this we noticed that the zero points of this curve coincided perfectly with the points of the grid we computed for the "2D grid" algorithm, which also coincided with the grid points of the grid used for the computation of the synthetic spectra. The deviation in between these grid points might be caused by different interpolation algorithms as the synthetic spectra are linearly interpolated from their grid whereas here we used a cubic spline interpolation. The cyan-marked data does not show this behaviour as nicely as the magenta one as the difference between them (see table 1) is the reddening mechanism at creation of the input synthetic magnitudes which is spectrum reddening for the cyan data. As mentioned before, using spectrum reddening for the fit function gives a systematic error, so it can be assumed that this holds for the use of spectrum reddening at the creation of the input synthetic magnitudes which would explain the "blurring".

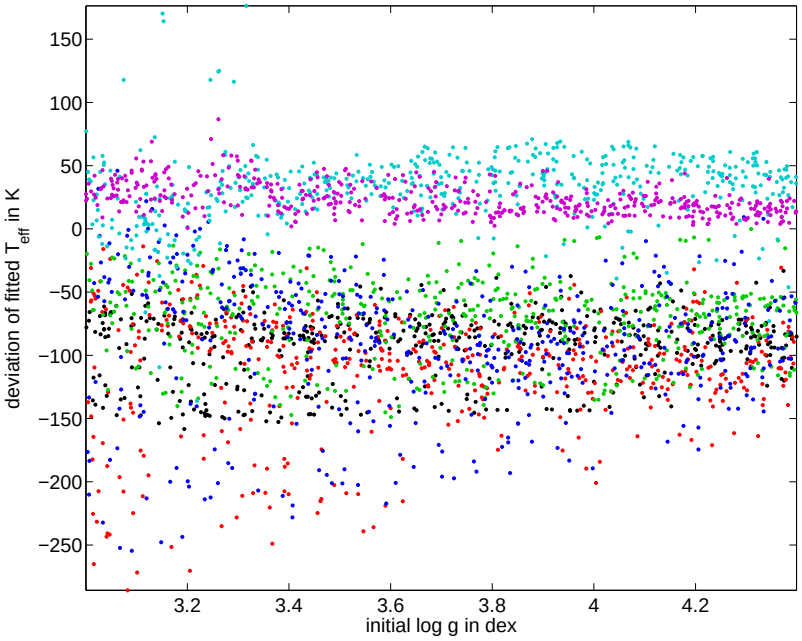

Figure 3: Obviously there is no significant dependence of the mistake in temperature estimation on the initial $\log g$ value.
Note that there is also no "sinusiodal" behaviour as in fig. 2. Thus seemingly the grid interpolation does not affect the fitting of the $\log g$ value significantly.

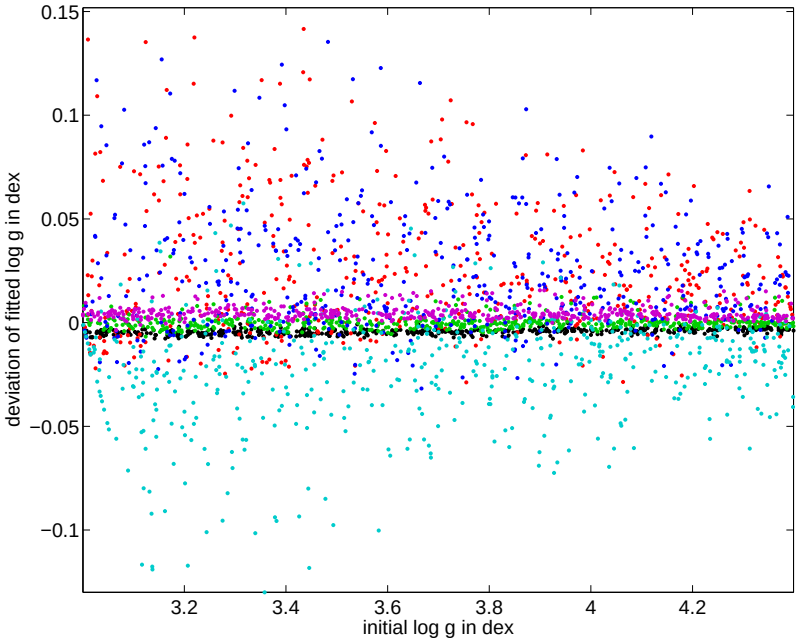

Figure 4: Deviation of the fitted $\log g$ from the initial values. Here we observe three trends: firstly there are three sets of data (black, green, magenta) that show a very good agreement with the initial values. Consulting table 1 one notices that these three datasets are the ones where the reddening mechanism used in the modelling of the input magnitudes is the same as the one used by the fit function (e.g. the input for the black data set was created using spectrum reddening and the "no grid" algorithm which also uses spectrum reddening).
The remaining three datasets both show a considerably bigger mismatch, where the red and blue data systematically overestimate $\log g$ whereas the cyan data systematically underestimates $\log g$. We notice that the red/blue and the cyan data are symmetric to each other (meaning that the picture is symmetric around the 0-axis).
As noted in figs. 2 and 3 the use of spectrum reddening brings in a systematic error. Seemingly for $\log g$ (contrary to T_eff) the systematic error by using spectrum reddening in the creation of the input synthetic magnitudes is the same (up to the sign) as the one made by use of spectrum reddening in the fit function. So if both times (at creation of the input magnitudes and at fitting time) the same reddening mechanism is used, the mistake cancels out giving a nearly perfect match (as for the three said datasets). If on the other hand the two available reddening mechanisms are mixed we make the mistake just once so it affects the data (with respective sign).
Also we note that here we do not see "sinusoidal" behaviour of any of the shown data. This empowers the interpretation in fig. 3 that the grid interpolation does not affect the fitting of the $\log g$ value.

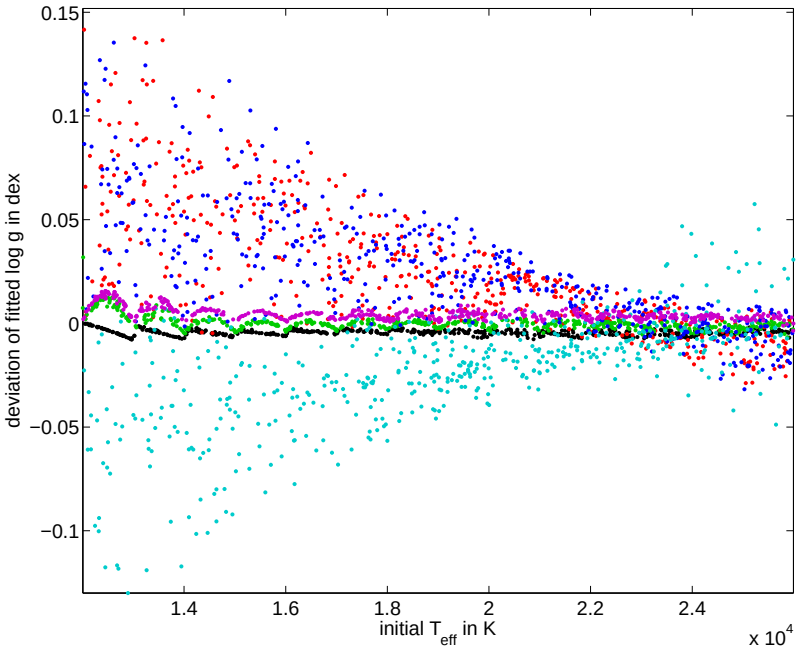

Figure 5: Deviation of $\log g$ plotted against initial $T_{\rm eff}$ value. Obviously the systematic error due to different reddening mechanisms (see fig. 4) is also dependent on $T_{\rm eff}$. Additionally here we see again the "sinusoidal" behaviour that we came across also in fig. 2, which once more reinforces the interpretation that the grid interpolation affects the fit.
But contrary to what one would expect we also see some strange systematic error in the black data, for which the "no grid" algorithm was used. This systematic error resembles the known "sinusoidal" behaviour, but is asymmetric. Of course the "no grid" algorithm still uses a grid to compute the synthetic spectra and the grid points of this grid also match the visible "jumps". But actually, as the fit also uses this grid, the error should cancel out. Thus unfortunately I can not explain this systematic error.

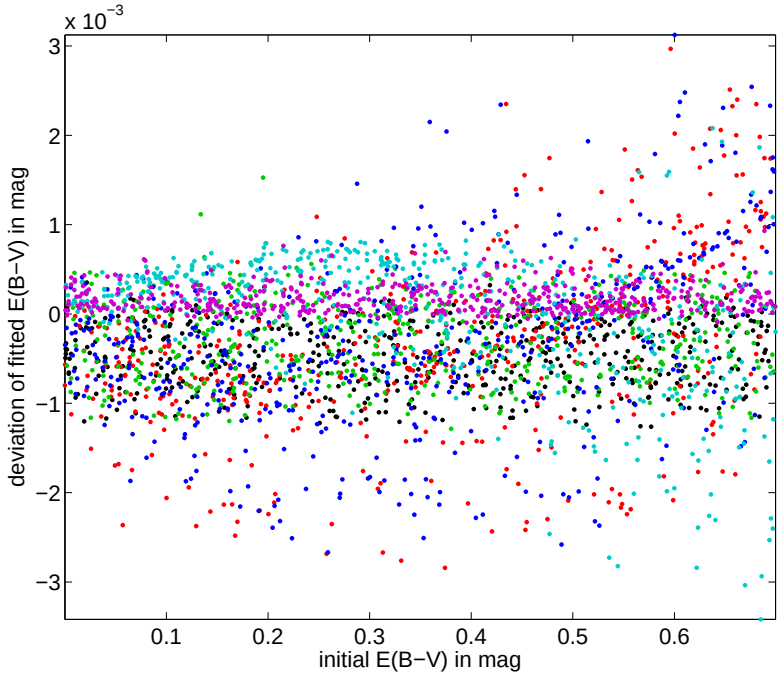

Figure 6: Deviation of $E(B-V)$ from the initial value. Here we see no significant dependence of the error on the initial value.

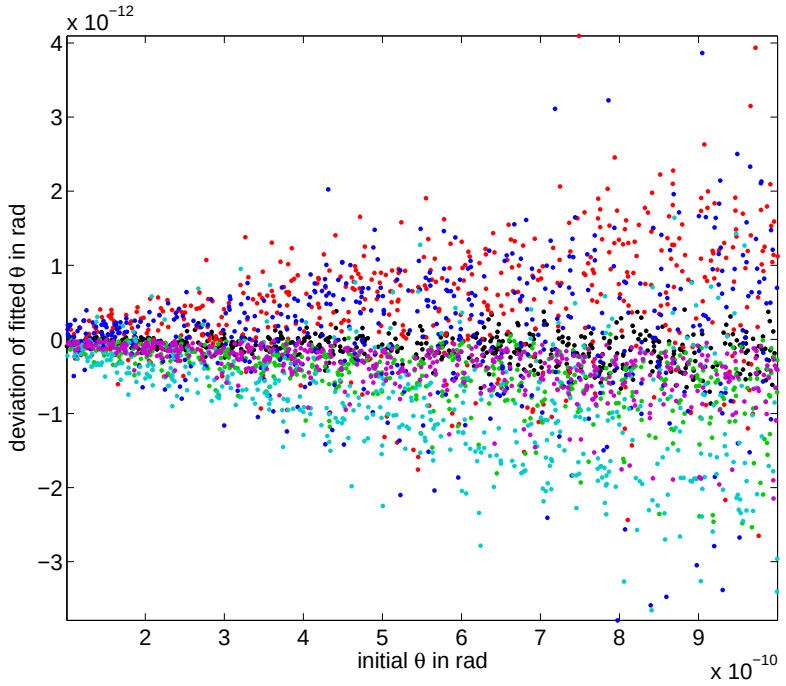

Figure 7: Deviation of θ from the initial value. Again (compare fig. 5) we see that the error is signed and thus the plot is symmetric.

5.3 $E(B-V)$ and θ

Obviously, $E(B-V)$ (fig. 6) and θ (fig. 7) mainly show the same trends as the plots before. Thus this will not be discussed further.

5.4 Conclusion

We have seen that the reddening mechanism and the grid interpolation have a significant influence on the goodness of the result. But one also has to see that these effects are small (relative errors around 10^{-2}). Thus the sole fact that we could discuss these small errors shows that overall the results are actually pretty good. Also as stated at the beginning, this program is meant to do a fast estimation of the stellar parameters for big samples of stars and is not intended for high precision computations.

References

M. Bessell and S. Murphy. Spectrophotometric Libraries, Revised Photonic Passbands, and Zero Points for UBVRI, Hipparcos, and Tycho Photometry. *PASP*, 124:140–157, February 2012. doi: 10.1086/664083.

E. L. Fitzpatrick. Correcting for the Effects of Interstellar Extinction. *PASP*, 111:63–75, January 1999. doi: 10.1086/316293.

R. Napiwotzki, D. Schoenberner, and V. Wenske. On the determination of effective temperature and surface gravity of B, A, and F stars using Stromgren UVBY beta photometry. *A&A*, 268:653–666, February 1993.